JUL 1 0 1987

CONF-870622--8

TITLE A HIGH-POWER RF LINEAR ACCELERATOR FOR FELS

AUTHOR(S) R. L. Sheffield, and J. M. Watson

SUBMITTED TO AIAA 19th Fluid Dynamics, Plasma Dynamics & Lasers Conference
June 8-10, 1987, Honolulu, Hawaii

MASTER

Los Alamos Los Alamos National Laboratory
Los Alamos, New Mexico 87545

DISTRIBUTION OF THIS

A HIGH-POWER RF LINEAR ACCELERATOR FOR FELS*

R. L. Sheffield and J. M. Watson
Los Alamos National Laboratory
Los Alamos, NM 87545

Abstract

In this paper we describe the design of a high average current rf linear accelerator suitable for driving short-wavelength free-electron lasers (FEL). We conclude that the design of a room-temperature rf linear accelerator that can meet the stringent requirements of a high-power short-wavelength FEL appears possible. The accelerator requires the use of an advanced photoelectric injector that is under development; the accelerator components, however, do not require appreciable development. At these large beam currents, low-frequency, large-bore room-temperature cavities can be highly efficient and give the specified performance with minimal risk.

Introduction

The design of a high average current rf linear accelerator suitable for driving short-wavelength free-electron lasers (FEL) is described. Some of the overall parameters are listed in Table 1. The high average current is necessary for conversion of the required average power to light by the FEL. A high peak current is needed to achieve high gain and a large conversion efficiency. The high gain is especially important in reducing the optical loading on the oscillator resonator mirrors. Higher gains allow more outcoupling, thereby reducing the circulating optical power within the resonator. Another critical parameter is the beam quality (emittance). For good energy-conversion efficiency at short wavelengths, the emittance growth of the electron beam must be minimized through all stages of acceleration and transport.

Table 1 Accelerator Parameters

Average current	1.75 A
Peak current	2000 A
Normalized emittance	< 100 π·mm·mrad
Resonant frequency	500 MHz
Charge per micropulse	28 nC
Micropulse repetition rate	62.5 MHz

The approach for achieving these stringent simultaneous requirements contains the following elements:

- A laser-gated photocathode, immersed in a high-gradient rf cavity, to produce high-quality electron bunches, which are quickly accelerated out of the space-charge-dominated energy range. The bunches require a further compression factor of only 4 to achieve the required peak current.
- A magnetic compression stage at 10 MeV to achieve electron bunching.

- Room-temperature accelerators, operated at 500 MHz, to maintain beam quality, to avoid beam breakup, and to utilize existing rf power sources. (Independent accelerating cavities are a good match to the power sources, are easily cooled, and provide redundancy in case of component failure.)
- Energy recovery of the residual electron-beam power to substantially reduce the rf power and electron beam dump requirements.

Photoelectric Injector

Introduction

Conventional injectors use a pulsed thermionic emitter of low peak brightness followed by a bunching, or phase compression, system that increases the peak current by a large factor. Ideally, the peak brightness should increase in proportion to the bunching factor; in reality, however, the result always falls short of the ideal. An additional shortcoming in the conventional type of buncher is that a repetition rate in excess of a few tens of megahertz is beyond the state of the art of electronically switched thermionic triode electron guns. Diode and triode guns have been operated in an rf cavity to produce electron pulses of width somewhat less than one-quarter of the rf period.[1-3] The ultimate upper limit to this technique for triode guns may be the power dissipation in the grid.

The required peak and average currents are clearly high and are beyond the capability of present conventional injector technology. With this understanding, Los Alamos has undertaken a program to develop a promising new type of injector called the laser photoelectric injector. The new development combines proven mode-locked lasers and semiconductor photoemitter electron sources. The point of departure of the Los Alamos innovation is the combination of proven technologies in a single entity, the rf-gun cavity.

Photocathode Emitter

In recent years, photocathodes for polarized electron sources have been made from wafers of GaAs.[4,5] Current densities as high as 180 A/cm^2 have been reported.[5] Photoemitters of cesium antimonide (Cs_3Sb) emit electrons in the subpicosecond to picosecond time range because of the short absorption depth of light.[6] By contrast, the intrinsic emission-time uncertainty of GaAs has been measured in the range from 8 to 71 ps for active layers between 50 nm and 2 μm in thickness.

A Cs_3Sb photocathode was chosen for its ease of preparation within the vacuum environment of the linac and for its relative tolerance to vacuum conditions in the injector linac.[7] A photoinjector linac must be bakeable in its entirety to about 200°C and must be capable of maintaining a pressure below 10^{-9} torr, preferably 10^{-10} torr. A damaged Cs_3Sb photocathode can be erased by heating to 400°C, then a new one is prepared in situ.

The spectral response[8] of Cs_3Sb includes quantum energies of doubled Nd:YAG (λ = 532 nm) and tripled (λ = 355 nm). A Nd:YAG laser can readily be mode-locked to deliver 60-ps pulse trains at a microscopic repetition rate in a range from 50 to 120 MHz.

In 1985, the achievement of high peak currents from a Cs_3Sb photocathode was reported.[9] Laser-driven Cs_3Sb photocathodes also have been used to produce an intrinsically bright beam;[10] more recently, these beams have been accelerated to relativistic energies without loss of brightness.

The Los Alamos Photoinjector Program

A proof-of-principle photoelectric gun is under development at Los Alamos.[11] The rf-gun cavity comprises a small-diameter Cs_3Sb photoemitter on the end wall of the cavity, frontally illuminated by an optical pulse train from a mode-locked Nd:YAG laser. The laser beam is directed along the electron beam axis of the linac. The high-intensity electric field in the rf cavity rapidly accelerates the electron bunch train, each bunch containing a high charge density. The initial rf-gun experiments are being carried out at a high frequency because a powerful klystron was available for use at 1300 MHz. A schematic diagram of the Los Alamos injector experiment is shown in Fig. 1.
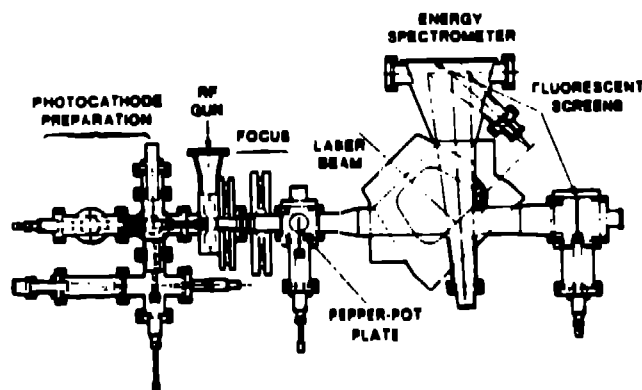

Fig. 1. The configuration of the first experiments includes a section for preparation of the photocathodes, on the left, the rf gun itself, and diagnostics in the form of an electron spectrometer and a pepper-pot plate.

Experiment Design

It is evident from simulation studies[12] of the acceleration of short bunches in an rf cavity that (a) dense space charge and (b) the external rf field lead to a degradation of beam quality and, therefore, to a loss of brightness. Although pulses of only a few picoseconds can be produced in a photocathode, it now seems advisable to generate pulses that are initially about 100 ps long and then to bunch them magnetically[13,14] at energies of above 10 MeV. The acceleration of the longer bunches is best done in a low-frequency linac to minimize emittance growth caused by variations in the rf field as the electron bunch exits the cavity. Nevertheless, the emittance improvement from an initial rapid acceleration drives the gradient higher, a condition that can only be met with high-frequency rf fields.[15] A study of the envelope equation[16] reveals that for continuous beams, the dominance of space charge over emittance is adiabatically damped as $\gamma^{1/2}$. For bunched beams, the damping dependence on energy is much stronger, namely γ^2.[17] Therefore, the requirement of maximum accelerating gradient (hence a high frequency) to minimize the influence of space charge must be balanced against a conflicting need to accept long pulses (hence a low frequency) to reduce the emittance growth associated with rf fields.

The acceleration rate in the rf-gun cavity is limited by the sparking breakdown characteristic of the cavity. A typical rf cavity that has been optimized

for maximum effective shunt impedance ZT^2 will have a ratio of peak surface electric field to average acceleration gradient[15] of about 4. A lower ratio, hence a larger maximum accelerating field, is obtained by decreasing the curvature of the beam-hole nose. Such a cavity is less efficient, but one gains a high acceleration rate with its use.

Jones and Peter[13] have shown that linear radial-electric fields in an accelerating cavity lead to a lower emittance growth for beams of uniform space-charge density. An rf-gun cavity designed for linear radial-electric fields automatically has a low ratio of peak surface field to average accelerating field. Therefore, an rf-gun cavity with linear electric fields in the beam region was chosen for this experiment.

In the Los Alamos photoinjector experiment, the chosen 1300-MHz cavity design had an effective shunt impedance $ZT^2 = 36$ MΩ/m. With a peak surface field of 60 MV/m (twice the nominal Kilpatrick breakdown field),[18] the average accelerating gradient is 30 MeV·m, a ratio of 2.0. The cavity power dissipation under maximum surface-field conditions is 0.6 MW.

After leaving the rf-gun cavity, the electron beam passes through two iron-shielded solenoid lenses as shown in Fig. 1. Between the two solenoids is a wall-current monitor (WCM) of the type used in the SLC (Stanford Linear Collider) injector.[19] The transverse emittance of the rf gun beam is measured by a pepper-pot plate that follows the solenoids. The pepper-pot method[20] uses an array of beamlets that samples the whole beam to map the transverse phase space. The beamlet formed in the pepper-pot plate (Fig. 1) drifts 80 cm to a quartz screen, where it is observed by a silicon-intensified vidicon. From a comparison of the measured spot size on the phosphor, with the beamlet obtained from an integration of the envelope equation, the transverse momentum of the beam is determined. The use of the envelope equation, which is valid for a continuous beam, is implicit in this method. The beamlet length-to-diameter aspect ratio is about 100; therefore, the approximation to a continuous beam is valid.

The temporal profile of the bunches is measured with a streak camera using the Cerenkov radiation from a pure quartz plate (Fig. 2). The Cerenkov light is collected by a planoconvex, f1.0 lens placed in contact with a quartz viewport. The collimated light is transported to the streak camera and focused onto the entrance slit with an overall magnification of 1/10. A sample of the laser-pulse light is merged with the electron beam's Cerenkov light by a 45° internally reflecting prism in the middle of the Cerenkov light

Fig. 2. Temporal profiles of the laser beam and photoelectron beam are measured on a single sweep in the streak camera.

beam, thereby eliminating the trigger jitter in the streak camera. The streak-camera sweep speed was calibrated using a variable path length for the laser light created by a movable retroreflector on an optical bench.

A double-focusing magnetic spectrometer is installed on the beamline. The dispersion on the detector plane is 0.8 cm/%, and the magnification is unity. With the aid of two solenoid lenses, a 20% momentum band can be analyzed. Alternatively, a 127-μm-diam hole can be scanned across a beam diameter at the object position (the pepper-pot plate) to do a differential momentum analysis. For this purpose, an intensified vidicon can view the detector plane through one of two viewports available.

Experimental Results

Initial observation of the accelerated electron beam from the rf gun was obtained with the WCM. With a fast oscilloscope, the largest pulse trains repeatedly observed had peak amplitudes of 4.4 V with 40 dB of attenuation in place. The measured bunch charge, obtained from the integrated pulse profiles, was 27 nC, giving an average current in the pulse train of 2.9 A. The measured temporal profile was Gaussian (see below), giving a peak current of 390 A. The probable error in these measurements was 20%. The peak observed current density was >600 A/cm².

The minimum laser pulse width observed was 53 ±1 ps FWHM; on the same streak-camera sweep, the electron bunch widths were the same to within the experimental error (Fig. 3). We conclude, therefore, that for the present experimental conditions, the pulse broadening introduced by the Cs_3Sb photoemission is less than 1 ps.

Accelerator

Following the rf photoinjector, the electron bunches are further accelerated to 10 MeV to stiffen the beam in preparation for magnetic compression. The electron bunches must be accelerated to moderately relativistic energies before compression because high-density pulses can be severely affected by the strong space-charge forces present. Before magnetic compression is used, the beam energy should be at least 10 MeV, a figure determined from PARMELA calculations. Magnetic compression uses a system of bending magnets designed to have path-length differences for particles of different momenta. Particles of lower momenta enter first and follow a shorter path than the path taken by the higher momenta particles that follow later. Thus, of necessity, the beam bunch must have an energy that is correlated in time. The lower the energy at which magnetic compression is used, the smaller the energy spread that must be corrected to meet the final energy-spread requirement. A magnetic compression located after 10-MeV initial acceleration gives a bunching factor of 4 (60 ps at 500 A to 15 ps at 2 kA) with an acceptable energy spread.

The remainder of the accelerator consists of independent room-temperature cavities with one 1 MW klystron per cavity. This section accelerates the 1.75-A beam from 10 MeV. Even with an enhanced bore of 10-cm diameter, the accelerator efficiency is approximately 94%. The average accelerating field within the cavities is 4.5 MV/m. This is high enough (2 MV/m over the length of the accelerator) to avoid cumulative beam breakup, yet low enough to make the cavity cooling manageable. Beam breakup at this average current can be avoided through the use of
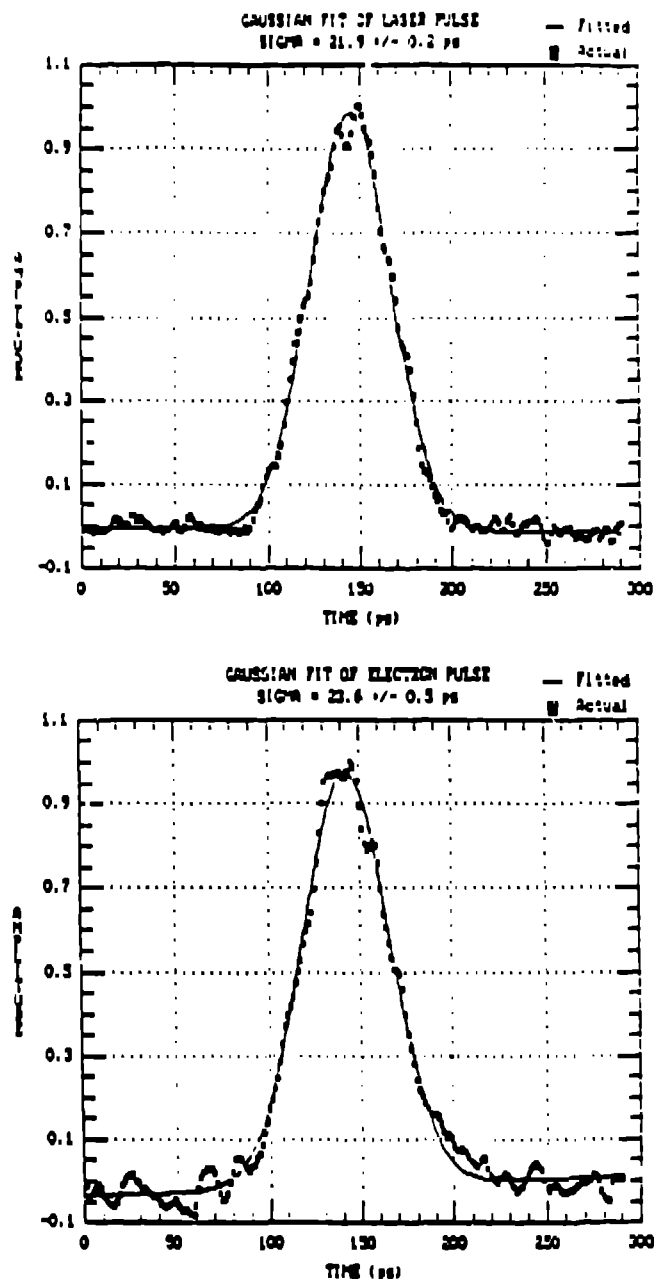

Fig. 3. Digitized streak-camera temporal profiles of the laser and photinjector beams.

staggered tuning (±1 MHz) of the dipole modes.[*] The peak current of 2000 A per micropulse is maintained throughout the linac. There should be little emittance growth in the linac with the moderate charge per pulse (28 nC). Every eighth bucket of the 500-MHz linac rf field contains a micropulse.

Energy recovery is incorporated by decelerating the beam in a parallel linac after bending the beam 180° and passing it through the undulator. A separate linac is required to allow optimization of the magnetic optics for the two very different beams and to avoid regenerative beam breakup. Each decelerating cavity is coupled to an accelerating cavity by a single cavity that absorbs very little power. Deceleration of the residual beam reduces the power required per

*K. Chan, Private Communication.

accelerating cavity from 1.7 to 0.6 MW. The amount of deceleration is limited by the energy spread imposed on the beam by a high-efficiency FEL. Energy recovery not only saves rf power, but it also greatly eases the power requirements of the electron-beam dump.

Summary

The design of a room-temperature rf linear accelerator that can meet the stringent requirements of a high-power short-wavelength FEL appears possible. The accelerator requires the use of an advanced photoelectric injector that is under development; the accelerator components, however, do not require appreciable development. At these large beam currents, low-frequency, large bore room-temperature cavities can be highly efficient and give the specified performance with minimal risk. The overall efficiency is improved by a factor of 2.2 by using an energy-recovery technique that was recently demonstrated at Los Alamos. FEL systems of greater power probably will consist of modules that will not be larger than this design.

References

1. S. P. Kapitza and B. N. Melekhin, *The Microton*, (Harwood Academic Publishers, London, Great Britain, 1978), p. 112.

2. D. E. Poole, T. R. Charlesworth, O. Gunnil, D. G. Peters, and G. Saxon, "An RF Modulated Electron Gun for NINA Injection Equipment," IEEE Trans. Nucl. Sci. 20 (3), 399 (1973).

3. G. A. Westenkow and J. M. J. Madey, Lasers and Particle Beams 2, 223 (1984).

4. D. T. Pierce, R. J. Gelotta, G. C. Wang, W. N. Uncrtl, A. Galens, C. E. Kuyatt, and S. R. Mielczarek, "GaAs Spin Polarized Electron Source," Rev. Sci. Instrum. 51, 478 (1980).

5. C. K. Sinclair and R. H. Miller, "A High Current, Short Pulse, RF Synchronized Electron Source for the Stanford Linear Collider," IEEE Trans. Nucl. Sci. 28 (3), 2649 (1981).

6. C. C. Phillips, A. E. Hughes, and W. Sibbett, "Photochron Streak Camera with GaAs Photocathode," in Ultrafast Phenomena IV, Eds., D. H. Auston and K. B. Eisenthal, (Springer-Verlag, Berlin, 1984) p. 420.

7. C. H. Lee, P. E. Oettinger, A Sliski, and M. Fishbein, "Practical Laser Activated Photoemissive Electron Source," Rev. Sci. Instrum. 56, 560 (1985).

8. W. E. Spicer, "Photoemissive, Photoconductive, and Optical Absorption Studies of Alkali-Antimonide Compounds," Phys. Rev. 112, 114 (1958).

9. C. H. Lee, P. E. Oettinger, E. R. Pugh, R. Klinkowstein, J. H. Jacob, J. S. Fraser, and R. L. Sheffield, "Electron Emission of Over 200 A cm² From a Pulsed-Laser Irradiated Photocathode," IEEE Trans. Nucl. Sci. 32 (5), 3045 (1985).

10. P. E. Oettinger, I. Bursuc, R. E. Shefer, and E. R. Pugh, "Brightness of an Intense Electron Beam Generated by a Pulse-Laser Irradiated Photocathode," Proc. 1987 Particle Accelerator Conf., Washington, D.C., March 16-20, 1987, to be published.

11. J. S. Fraser, "Photocathodes in Accelerator Applications," Proc. 1987 Particle Accelerator Conf., Washington, D.C., March 16-20, 1987, to be published.

12. M. E. Jones and W. K. Peter, "Particle-in-Cell Simulations of the Lasertron," IEEE Trans. Nucl. Sci. 32 (5), 1794 (1985).

13. M. E. Jones and W. K. Peter, "Theory and Simulation of High-Brightness Electron Beam Production From Laser-Irradiated Photocathodes in the Presence of DC and RF Electric Fields," Proc. 6th Int. Conf. on High-Power Particle Beams, Kobe, Japan, 1986, to be published.

14. J. S. Fraser, "Electron Linac Injector Developments," 1986 Linac Conf. Proc., Stanford Linear Accelerator Center report SLAC-303, 411 (1986).

15. S. O. Schriber, "Factors Limiting the Operation of Structures Under High Gradient," 1986 Linac Conf., Proc. Stanford Linear Accelerator Center report SLAC-303.

16. J. D. Lawson, The Physics of Charged Particle Beams, (Oxford University Press, Oxford, Great Britain, 1977), p. 134.

17. M. E. Jones and B. E. Carlsten, "Space-Charge Induced Emittance Growth in The Transport of High-Brightness Electron Beams," Proc. 1987 Particle Accelerator Conf., Washington, D.C., March 16-20, 1987 to be published.

18. W. D. Kilpatrick, "Criterion for Sparking Designed to Include Both RF and DC," Rev. Sci. Instrum. 28, 824 (1957).

19. M. B. James, J. E. Clendenin, S. D. Ecklund, R. H. Miller, J. C. Sheppard, C. K. Sinclair, and J. Sodja, "Update on the High-Current Injector for the Stanford Linear Collider," IEEE Trans. Nucl. Sci. 30 (4), 2992 (1983).

20. C. LeJeune and J. Aubert, "Emittance and Brightness: Definitions and Measurements," in Applied Charged Particle Optics, Ed., A. Septier, Advances in Electronics and Electron Physics, Supp. 13A (1980).